https://doi.org/10.5194/egusphere-2026-2665
Preprint. Discussion started: 13 July 2026

Cascading Wildfire–Atmospheric River Hazards: Postfire Flood Risk after the 2025 Eaton Fire

Fehmida Rafi[1], Daniel Rowland[1], Shang Gao[1]

[1]School of Natural Resources and the Environment, University of Arizona, Tucson, 85721, United States

Correspondence to: Shang Gao (shanggao@arizona.edu)

Abstract. Wildfires and extreme precipitation events increasingly interact under a warming climate, yet their combined hydrologic impacts remain poorly characterized. In fire-prone regions such as Southern California, atmospheric rivers (ARs) can both promote wildfire through antecedent vegetation growth and trigger severe flooding in postfire landscapes. This study evaluates the compound flood risk associated with a strong AR event occurring after the 2025 Eaton Fire by examining both its likelihood and hydrologic consequences. Historical AR records were analyzed to assess the probability of sequential-year strong AR events, and an event-based hydrologic modeling framework (AGWA/KINEROS2) was used to characterize watershed response under prefire and postfire conditions using precipitation analogous to the February 2024 AR. Results indicate that strong AR events (Scale $\geq$ 3) occur with a mean annual frequency of 0.51 and a 38% probability of recurrence in consecutive years, supporting the plausibility of a postfire AR scenario. Simulations show that wildfire-induced landscape changes amplify downstream flood response, increasing runoff volume by approximately 6% and sediment yield by about 50% in channels immediately below the burned area. Sequential storm pulses further enhanced postfire impacts, with the second flood peak increasing by ~30% relative to prefire conditions. These findings demonstrate that wildfire and AR events act as interconnected hazards whose cascading effects can intensify flood and erosion risks. By linking event probability with watershed-scale hydrologic response, this study provides a framework for assessing postfire flood hazards under compound climate extremes and underscores the need for integrated risk management in fire-affected regions.

1 Introduction

Wildfires are becoming more frequent, larger, and more destructive across many regions of the world. Although large historical events such as the 1910 Big Burn in the Northern Rockies shaped early fire management in the United States, recent decades have witnessed wildfires of unprecedented scale, intensity, and socio-economic impact, including major events in Canada (2016), Chile, Portugal and the United States (2017), Northern Europe and South Africa (2018), Bolivia (2019), and Australia and the United States (2020)(Duane et al., 2021). Climate change, particularly increasing temperatures, prolonged drought, and more extreme fire weather, has emerged as a primary driver of these trends. In addition, anthropogenic factors such as altered forest structure, fuel accumulation, and land management practices further exacerbate fire severity and spread(Keeley

https://doi.org/10.5194/egusphere-2026-2665
Preprint. Discussion started: 13 July 2026

and Syphard, 2021; Abatzoglou et al., 2023; Kelley et al., 2025). These trends are expected to intensify in the future, resulting in more frequent and severe fire weather conditions and longer fire seasons(Kumar et al., 2025). While controlled fire can play an ecological role in ecosystem renewal, highly destructive large wildfires pose substantial risks to human health, infrastructure, water resources, and downstream communities(Carlson et al., 2025).

The western United States particularly California has a long history of large wildfires, including the approximately 100,000 ha Santiago Canyon Fire of 1889 in Orange County as well as the Matilija Fire of 1932 and the Laguna Fire of 1970. In the past four decades, the number of fires exceeding 10,000 ha, with several surpasses 100,000 ha have been increased, resulting in loss of life and property(Keeley and Syphard, 2021). The largest fires on record occurred in 2018, Camp Fire followed by even larger event in 2021, the Dixie Fire(Dilshan et al., 2025). The large fires in the past were low intensity surface fires whereas, the recent ones are dominated by high intensity crown fire.

In 2025, Southern California experienced the most destructive wildfires, the Los Angeles County's Palisades and Eaton Fires(Phillips, 2025). On January 07, 2025, Eaton Fire ignited on the eastern hillside of the Eaton Canyon Wash in Los Angeles County, Southern California along the foothills of the San Gabriel Mountains, a landscape characterized by steep canyons, dense evergreen forests, and extensive chaparral. This terrain, combined with highly flammable vegetation, makes the region inherently susceptible to rapid fire spread. In the months preceding the fire, Southern California experienced approximately eight months without significant precipitation, leading to extremely low antecedent soil moisture and elevated vegetation dryness. Despite this prolonged dry period, a strong Atmospheric River (AR) event in 2024 delivered substantial precipitation, promoting vigorous vegetation growth and increasing available fuel loads. These accumulated fuels later became highly combustible under renewed dry conditions. Fire risk was further amplified across the steep terrain by powerful Santa Ana winds where downslope, dry wind events that are historically associated with some of the most destructive wildfires in California(Guirguis et al., 2023; Abatzoglou et al., 2023). Over the past four decades, California has experienced an approximate 1°C increase in temperature and a ~30% decline in precipitation, trends that have contributed to more frequent and severe Santa Ana wind-driven fires(Keeley et al., 2021). Thus, the combination of prolonged drought, fuel accumulation following the AR event, and extreme wind conditions combinedly led to the rapid ignition and spread of the Eaton Fire.

Wildfires substantially alter watershed structure and function, directly affecting hydrologic processes such as infiltration, runoff generation, streamflow response, and sediment transport. The combustion of vegetation and soil organic matter reduces canopy interception, surface roughness, and root reinforcement, while high soil temperatures can induce water-repellent (hydrophobic) layers. As a result, postfire landscapes exhibit reduced infiltration capacity and diminished water storage. Previous studies reported that surface runoff can increase by more than 70%, while erosion rates may rise by orders of magnitude following high-severity fires(Papaioannou et al., 2023; Sidman et al., 2016; Samburova et al., 2023; Prats et al., 2021; Moazeni and Cerdà, 2024). Therefore, wildfires like Eaton fire can change the characteristics of the watershed by reducing the vegetation cover, increasing hydrophobic layer, and changing the surface condition, which can pose serious risks such as increase in surface runoff and erosion in the downstream areas.

https://doi.org/10.5194/egusphere-2026-2665
Preprint. Discussion started: 13 July 2026

Atmospheric rivers (AR) are long narrow rivers in the lower atmosphere that carry significant amounts of moisture from tropical to the high latitude regions. In California, ample precipitation is delivered by landfalling ARs particularly during boreal winter, responsible for up to half of the state's annual precipitation(Corringham et al., 2022; Gershunov et al., 2017). The interaction of AR moisture plumes with California's complex topography enhances orographic precipitation, frequently producing heavy rainfall and flooding(Cobb et al., 2022; Gershunov et al., 2017). Although AR frequency varies from dry to wet years, a small number of intense, long-duration ARs often determines whether a season is drought- or flood-dominated. During the 2022-2023 and 2023-2024 water years, multiple AR events ended the two-decade megadrought, making them the two wettest consecutive years in California's recorded history(Selby, 2025). In winter 2022-2023 alone, 31 AR events impacted the state, replenishing reservoirs but also triggering widespread floods, landslides, and debris flows across 47 counties. In February 2024, one of the most intense AR events on record delivered more than 8 inches of rainfall across parts of the Los Angeles Basin, which accounts for over half the region's average annual precipitation and caused extensive flooding and hundreds of debris flows(Selby, 2025).

California is already experiencing pronounced interannual variability in precipitation and hydrometeorology, and climate change is projected to further intensify extreme events, including droughts, wildfires, and Atmospheric Rivers (ARs). Importantly, these hazards do not occur in isolation. The Intergovernmental Panel on Climate Change (IPCC) Sixth Assessment Report (AR6) emphasizes that the probability of compound and cascading climate events will increase under continued warming(Qing et al., 2023). In California, prolonged drought and record-high temperatures often precede large wildfires, while intense AR events following wildfire can trigger severe postfire flooding, debris flows, and landslides(Guirguis et al., 2023; Miller et al., 2025; Aghakouchak et al., 2018). This fire-precipitation sequence illustrates a compounding hazard pathway: dry, warm, and windy conditions elevate wildfire risk and promote soil hydrophobicity, thereby increasing watershed sensitivity to subsequent heavy rainfall. Conversely, AR events can enhance vegetation growth on interannual timescales, increasing fuel availability and shaping future fire behavior(Albano et al., 2017). The Eaton Fire exemplifies this cascading risk. A strong AR event in February 2024 enhanced vegetation growth in Southern California, followed by an extended dry period that reduced soil moisture and desiccated fuels, increasing wildfire susceptibility. Should a similarly intense AR event occur following the 2025 Eaton Fire, the downstream flood hazards could be substantially amplified via altered watershed conditions including reduced vegetation cover and increased soil water repellence.

Despite growing recognition of such cascading wildfire-storm interactions, there is still lack of research to explicitly quantify the compound risk. In this study, we frame such risk through its two components: (1) the likelihood of a strong AR event occurring after a major wildfire, and (2) the resulting hydrologic consequences. To this end, this study quantifies the postfire flood impact of the 2025 Eaton Fire under a strong AR scenario analogous to the February 2024 event. We first assess the frequency and recurrence characteristics of historical intense ARs in Southern California to evaluate the likelihood of such a scenario. We then apply a hydrologic modelling framework to estimate and characterize the flood impact attributable to wildfire-induced changes in watershed properties. The remainder of this paper is organized as follows: Section II describes the study area and methodology; Section III presents the results; Section IV discusses the implications; and Section V concludes.

https://doi.org/10.5194/egusphere-2026-2665
Preprint. Discussion started: 13 July 2026

2 Materials and Methods

This section outlines the framework used to evaluate postfire flood potential in the Eaton-Santa Anita watershed under extreme precipitation forcing. We first describe the study area and characterize the February 2024 Atmospheric River (AR) event that serves as a representative rainfall scenario. We then assess the frequency and recurrence of strong AR events to establish the plausibility of similar future conditions. Finally, we apply the AGWA/KINEROS2 modeling framework, incorporating postfire landscape changes and addressing observational constraints through volume-based calibration, to quantify runoff response under prefire and postfire conditions.

2.1 Study Area

The study focuses on two adjacent HUC-12 watersheds, i.e., Arroyo Seco and Eaton-Santa Anita (ESA), located along the southern foothills of the San Gabriel Mountains in Los Angeles County, California (Fig. 1). Both watersheds drain steep mountainous headwaters into densely urbanized areas of Altadena and Pasadena, connecting fire-impacted uplands and downstream developed communities. In January 2025, the Eaton Fire ignited near Eaton Canyon and burned extensively across the upper elevations of both watersheds. Between the two basins, the ESA watershed was more severely impacted, containing approximately 82.4% of the total burned area. The spatial distribution of burn severity, derived from the Burned Area Reflectance Classification (BARC) map developed by the Burned Area Emergency Response (BAER) team, indicates that 74.3% of the burned landscape experienced moderate severity, followed by 17.1% low severity, 4.0% high severity, and 4.6% unburned to very low severity. In terms of hydrology, the concentration of burn severity in the headwater regions is of particular importance, as these areas are critical sources of runoff and sediment delivery to downstream channels. Despite the lesser burn severity, the Arroyo Seco watershed was selected due to the only operational USGS stream gauge in the region, which provides streamflow observations for hydrologic model calibration and validation.

https://doi.org/10.5194/egusphere-2026-2665
Preprint. Discussion started: 13 July 2026

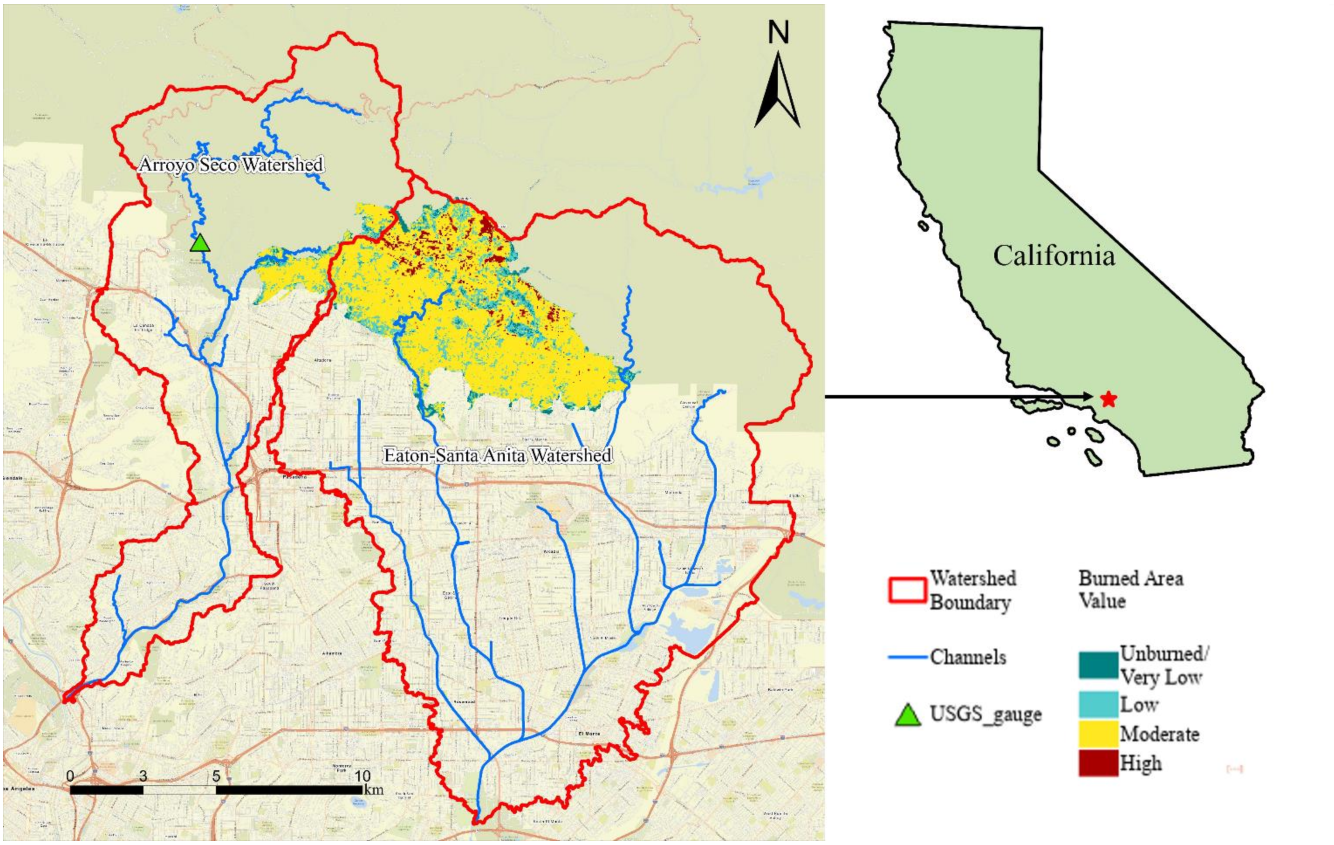

Figure 1: Map of the study area showing the Arroyo Seco and Eaton-Santa Anita (ESA) watersheds, burn severity from the Eaton Fire based on the Burned Area Reflectance Classification (BARC), and the location of the USGS stream gauge (ID: 11098000) used for hydrologic model calibration.

In early February 2024, California was impacted by a severe Atmospheric River (AR) that delivered intense precipitation, strong winds, and widespread flooding across the state. Over a three-day period, more than 7-8 inches (≈180-200 mm) of rainfall accumulated across the Los Angeles Basin, while adjacent mountain slopes received over 300 mm (>1 ft) of precipitation. Within this short duration, numerous weather stations recorded rainfall totals equivalent to nearly half of the region's average annual precipitation, triggering hundreds of mudslides and debris flows(Selby, 2025). Figure 2 shows the spatial distribution of cumulative precipitation associated with this AR event, derived from the Analysis of Record for Calibration (AORC) dataset. Between 1 February and 9 February 2024, the study watersheds received approximately 300-399 mm of total rainfall, with higher accumulations observed in the mountainous headwater regions. This event provides a representative extreme precipitation scenario capable of mobilizing runoff and sediment from fire-affected landscapes

https://doi.org/10.5194/egusphere-2026-2665
Preprint. Discussion started: 13 July 2026

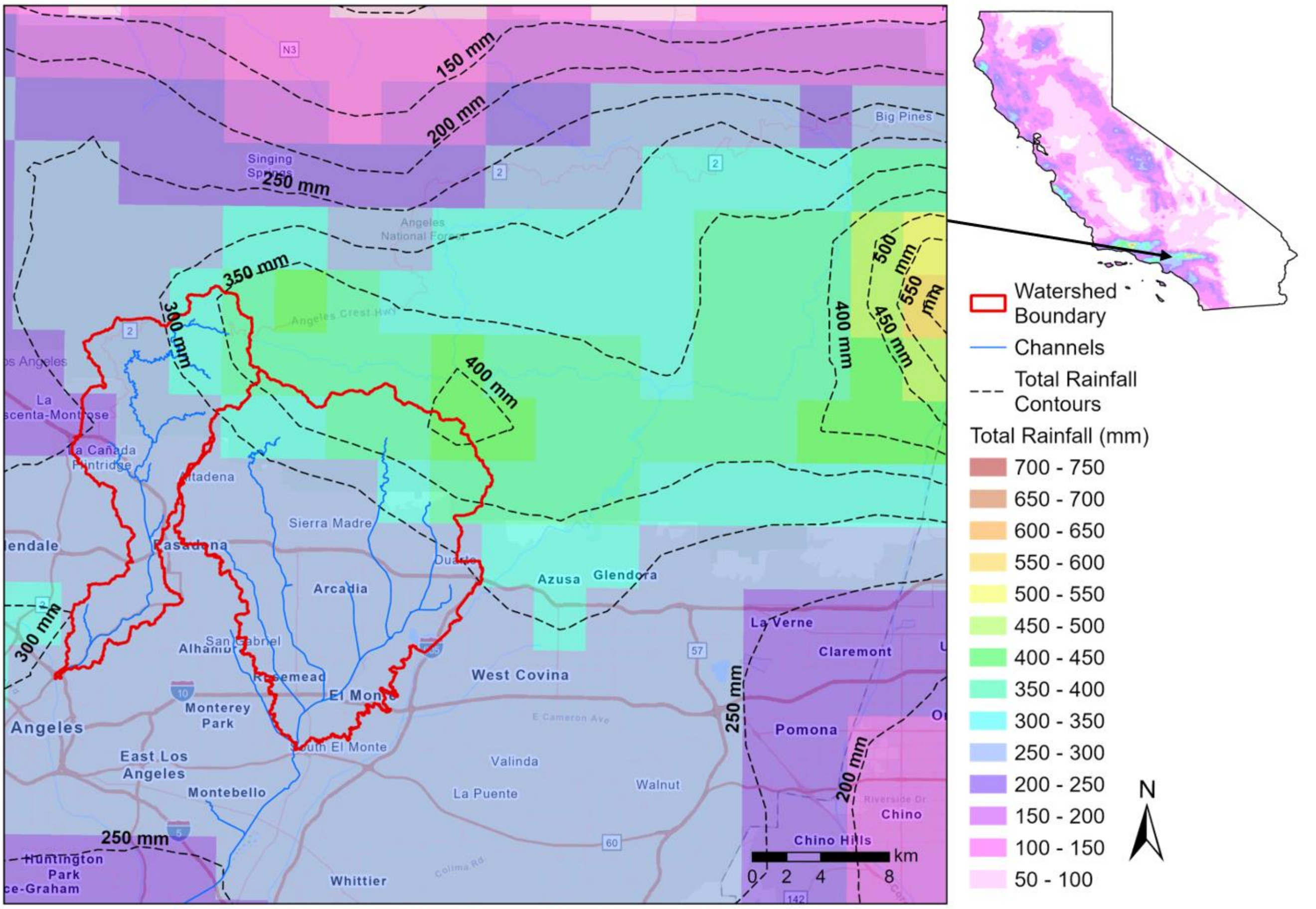

Figure 2: Spatial distribution of cumulative precipitation from the February 2024 Atmospheric River event across the study watersheds, based on AORC data, indicating 300-399 mm of rainfall between 1-9 February 2024.

2.2 Frequency and Recurrence Analysis of the February 2024 AR Event

To assess the plausibility of a strong Atmospheric River (AR) event occurring in the year following the 2025 Eaton Fire, we quantified both the frequency and conditional recurrence of intense AR events in Southern California. This analysis provides context for evaluating the likelihood of an extreme precipitation event capable of triggering postfire flooding and erosion. We used the CW3E Coastal Landfalling AR Catalog, a scale for characterizing the strength and impacts of ARs introduced by Ralph et al. (2019). The catalog identifies AR events on a 0.5° × 0.5° grid along the U.S. West Coast and classifies their intensity using the AR Scale, which is based on vertically integrated water vapor transport (IVT) and event duration (Ralph et al., 2019) The February 2024 event was classified as an AR3 (Category 3) event, representing a strong AR. In this study, we define frequency as the average annual occurrence of strong AR events (AR Scale $\geq$ 3). We define recurrence as the conditional probability of at least one strong AR event occurring in a given year, provided that a strong AR event occurred in the preceding year. This metric captures the likelihood of AR events in the sequential, which is directly relevant to the hypothesized scenario

https://doi.org/10.5194/egusphere-2026-2665
Preprint. Discussion started: 13 July 2026

of an AR following the Eaton Fire. Using the 65-year CW3E record (1960-present), we selected five coastal grid locations near the study watersheds to evaluate the frequency and recurrence characteristics of AR3-or-greater events.

2.3 Hydrologic Modelling

Hydrologic modeling provides a practical means to quantify the impact of wildfire-induced landscape changes on runoff generation and sediment transport, thereby supporting flood risk assessment and watershed management. In this study, we applied the AGWA/KINEROS2 modeling framework to simulate postfire runoff and erosion response in the Eaton-Santa Anita (ESA) watershed under extreme precipitation forcing. AGWA (Automated Geospatial Watershed Assessment) serves as a GIS-based parameterization tool that prepares spatial inputs for hydrologic models using terrain, land cover, and soil datasets, while the KINEROS2 (K2) model functions as the simulation engine that computes event-based runoff and sediment transport across discretized hillslope and channel elements.

2.3.1 Automated Geospatial Watershed Assessment (AGWA)

AGWA integrates geospatial datasets, including digital elevation models (DEM), land cover, and soil properties, to automate watershed delineation, discretization, and parameterization(Goodrich et al., 2012). The datasets used for model setup, input forcing, and calibration are summarized in Table 1. In this study, a 10-m USGS DEM was used to delineate the watersheds. Using a 3% flow accumulation threshold along with a burnt-in National Hydrography Dataset High Resolution (NHD-HR) flowline, the ESA watershed was discretized into 47 hillslopes and 19 channels, while the Arroyo Seco watershed was discretized into 55 hillslopes and 22 channels. Land use parameters were derived from the National Land Cover Dataset (NLCD-23), and soil properties were obtained from the gridded Soil Survey Geographic Database (gSSURGO). To represent postfire conditions, AGWA modifies key surface parameters, including Manning's roughness coefficient, saturated hydraulic conductivity, and canopy interception, based on burn severity from the Burned Area Reflectance Classification (BARC). These adjustments are implemented through pixel-level lookup tables and subsequently aggregated to hillslope and channel scales.

2.3.2 KINEROS2 (K2) Model

KINEROS2 is an event-based distributed hydrologic model that simulates runoff and sediment transport across hillslopes and channel networks(Goodrich et al., 2012). The watershed is conceptualized as a system of interconnected elements in which outflow from upstream hillslopes or channels becomes input to downstream elements. Although AGWA was used for parameterization, simulations were conducted directly in KINEROS2 to allow multi-day event modeling beyond AGWA's 24-hour runtime limitation. The February 2024 AR event was simulated using precipitation data from the AORC dataset. Hourly 1-km gridded rainfall was spatially averaged for each hillslope and applied as time-series forcing to the model. To represent antecedent dry conditions following the prolonged eight-month rain-free period preceding the Eaton Fire, the initial soil saturation was set to 0.001. Simulations were performed over the full duration of the AR event from 1-9 February 2024

https://doi.org/10.5194/egusphere-2026-2665
Preprint. Discussion started: 13 July 2026

(12,960 minutes) using a 5-minute time step based on Courant stability criteria. Both prefire and postfire scenarios were evaluated.

Table 1: Datasets used for model setup, forcing, and calibration

Purpose	Name	Resolution	Source
Input forcing	Analysis of Record for Calibration (AORC)	~ 4 km, hourly	National Oceanic and Atmospheric Administration (Aorc, n.d.)
Model setup	Digital Elevation Model	10 meters	United States Geological Survey (Usgs, n.d.–a)
	National Land Cover Database of 2023	30 meters	United States Geological Survey (Mrlc, n.d.)
	Gridded Soil Survey Geographic (gSSURGO)	10 meters	Natural Resources Conservation Service (Gssurgo, n.d.)
	Burned Area Reflectance Classification (BARC)	30 meters	Burned Area Emergency Response (Baer, n.d.)
Model Calibration	USGS streamflow	15 minutes	United States Geological Survey (Usgs, n.d.–b)

2.4 Model Finetuning

The Eaton-Santa Anita (ESA) watershed lacks continuous streamflow observations suitable for calibration. The only available USGS gauge in the region (ID: 11098000) is located in the adjacent Arroyo Seco watershed (Fig. 2). This gauge is positioned immediately downstream of the Brown Mountain Dam, a structure built in the 1940s that is no longer operational and is now filled with sediment. Flow passing over the sediment-filled dam experiences a substantial drop of approximately 25 meters into a downstream plunge pool, resulting in significant dissipation of kinetic energy. As a result, the recorded hydrograph is hydraulically attenuated and does not preserve the flash response characteristics typical of steep headwater basins, such as sharp peak flows and rapid rising limbs. Consequently, the sub-hourly discharge observations at this location do not fully represent the true event-scale flood dynamics upstream.

To address this limitation, the 15-minute discharge record was aggregated to event total value for calibration purposes. Similarly, model simulations were still performed at the native 5-minute temporal resolution but were subsequently aggregated to event total value for comparison with observations. This approach prioritizes accurate representation of runoff volume while avoiding misinterpretation of peak discharge magnitude or timing, which are dampened by hydraulic attenuation at the gauge location. Given that the primary objective of this study is to quantify changes in watershed-scale runoff response under postfire

https://doi.org/10.5194/egusphere-2026-2665
Preprint. Discussion started: 13 July 2026

conditions, volume-based calibration provides a physically meaningful constraint despite the limitations of the observational record.

3 Result

This section presents the outcomes of the hydrologic modelling analysis under both prefire and postfire conditions. We first evaluate the frequency and recurrence characteristics of strong Atmospheric River (AR) events to establish the plausibility of the modelled scenario. We then assess model calibration performance and examine spatial variability in runoff response across the study watersheds. Finally, we compare prefire and postfire hydrologic and sediment responses to quantify how wildfire-induced landscape changes influence flood peaks, runoff generation, and sediment yield.

3.1 Frequency and Recurrence Analysis of the February 2024 AR Event

Figure 3 summarizes the frequency and conditional recurrence of strong Atmospheric River (AR $\geq$ 3) events at five coastal locations in Southern California. Each location represents a 0.5° × 0.5° grid cell from which AR characteristics were extracted. Although the February 2024 AR event exhibited spatially variable intensity across these locations (ranging from AR1 to AR3 depending on local IVT magnitude and duration), the analysis here focuses on the historical occurrence of strong AR events (AR $\geq$ 3). Across the 64-year record (1960-2024), the mean frequency of AR $\geq$ 3 events is 0.51 events per year across the five locations, with values ranging from 0.34 to 0.83 events per year. The conditional recurrence, defined as the probability of a strong AR event occurring in a given year following at least one such event in the previous year, averages 38%, with values ranging from 30% to 56%. These results indicate that strong AR events occur intermittently but not infrequently in Southern California, and that sequential-year occurrences are reasonably likely. Consequently, the occurrence of a strong AR event following the Eaton Fire, as hypothesized in this study, is supported by historical AR behavior, with an estimated conditional probability of approximately 38%.

https://doi.org/10.5194/egusphere-2026-2665
Preprint. Discussion started: 13 July 2026

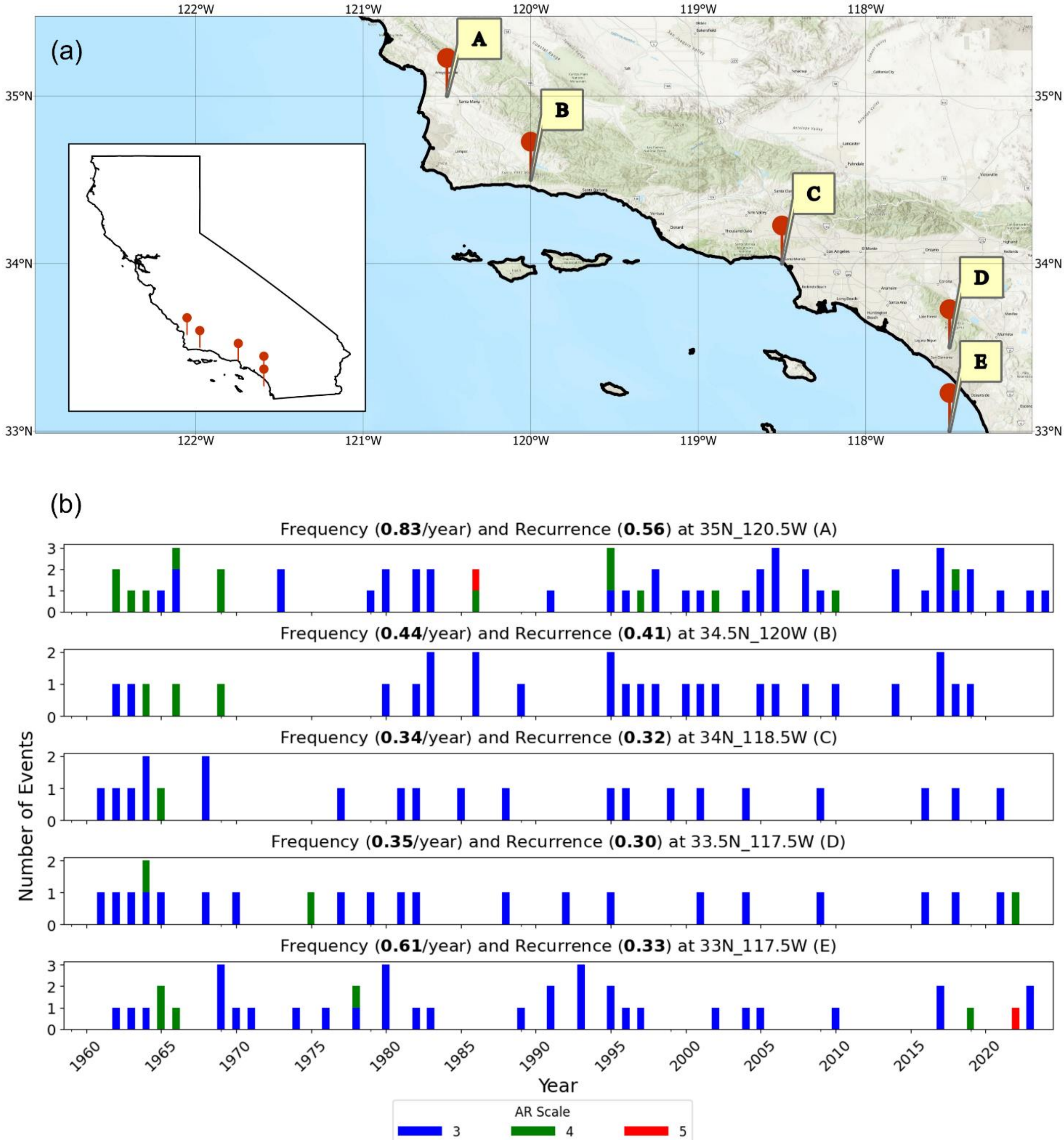

Figure 3: Frequency and conditional recurrence of strong Atmospheric River events (AR ≥ 3) at five coastal locations in Southern California: A (35°N, 120.5°W), B (34.5°N, 120°W), C (34°N, 118.5°W), D (33.5°N, 117.5°W), and E (33°N, 117.5°W). AR events were identified within a 0.5° × 0.5° grid centered at each location. Annual counts of AR ≥ 3 events from 1960 to 2024 are shown for each site.

https://doi.org/10.5194/egusphere-2026-2665
Preprint. Discussion started: 13 July 2026

3.2 Hydro-Modelling Results - Model Finetuning

For the AR-driven flood event from 1-9 February 2024, key hydrologic parameters, we calibrate the model by adjusting watershed-scale multipliers on key hydrologic parameters including saturated hydraulic conductivity, coefficient of variation of Ksat, and capillary drive coefficient. This calibration resulted in near-zero bias in total event runoff volume at the Arroyo Seco gauge, i.e., 10% of runoff coefficient from both simulation and observation. Figure 4 presents the calibrated runoff coefficients for hillslope elements across both watersheds. Hatched areas denote the contributing drainage area (42 km^2) to the USGS gauge in the Arroyo Seco watershed, along with a comparable cumulative contributing area identified within the ESA watershed for consistency in comparison. The box plot illustrates runoff coefficient distributions for these contributing areas. The area-weighted mean runoff coefficient is 9.87% in the Arroyo Seco watershed and 11.7% in the ESA watershed, indicating broadly similar runoff responses under calibrated prefire conditions. Spatial variability in runoff coefficients reflects underlying soil characteristics. Lower values are associated with sandy soils that promote infiltration (e.g., Plane 23, 52 and 61 in ESA watershed and Plain 63 in Arryo Seco watershed), whereas higher runoff coefficients occur in loamy soil regions where infiltration capacity is reduced (e.g., Planes 11, 31, and 62 in ESA and plane 32 in Arroyo Seco).

https://doi.org/10.5194/egusphere-2026-2665
Preprint. Discussion started: 13 July 2026

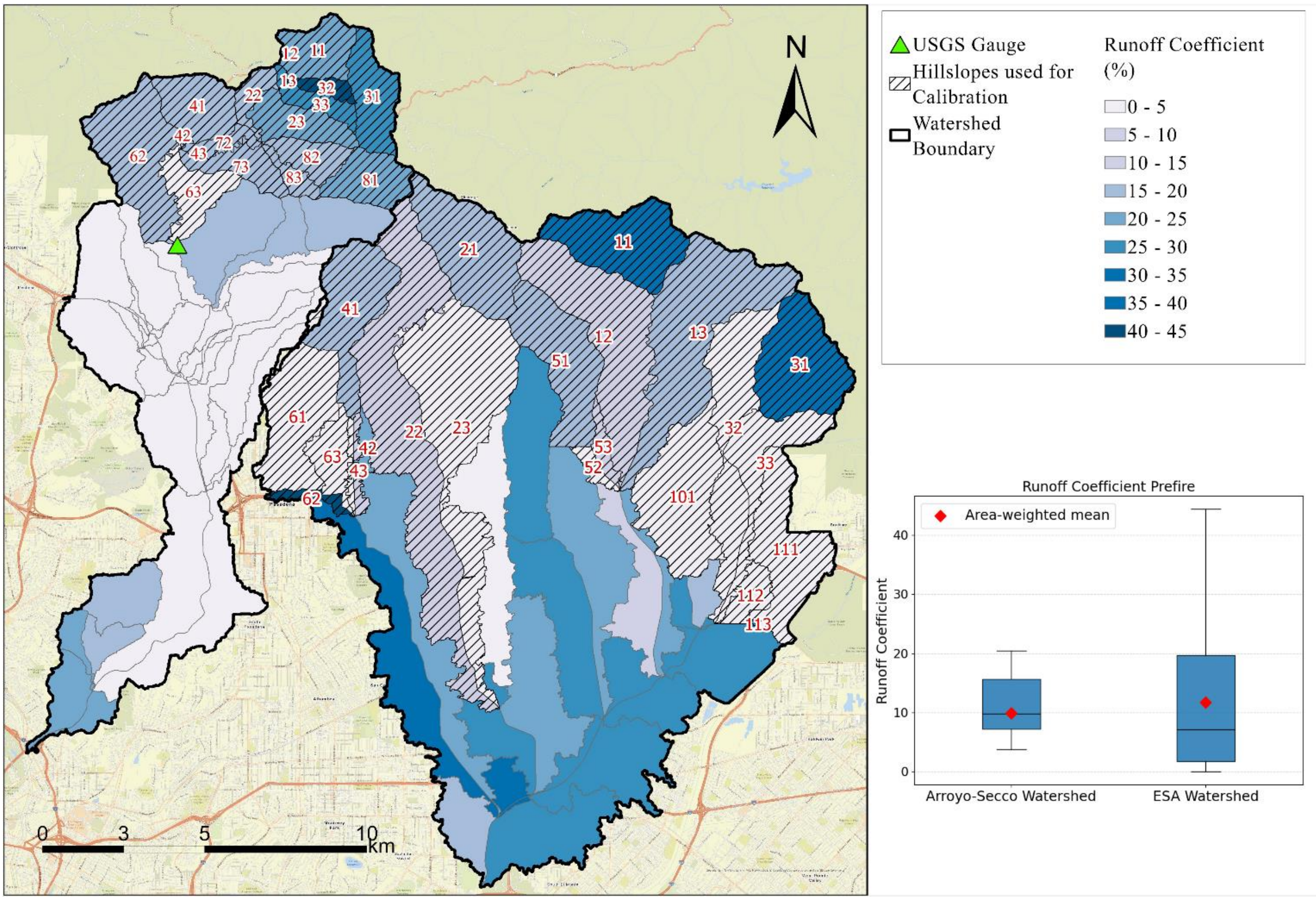

Figure 4: Spatial distribution of prefire runoff coefficients across the Arroyo Seco and Eaton–Santa Anita (ESA) watersheds. Hatched areas indicate hillslopes contributing to the USGS gauge in the Arroyo Seco watershed and a comparable cumulative area in the ESA watershed used for calibration and comparison. The accompanying boxplot summarizes runoff coefficient distributions within these hatched areas, with red diamonds representing area-weighted mean values.

3.3 Hydro-Modelling Results - Prefire and Postfire Comparison

Following calibration, AGWA-K2 simulations were conducted to represent both prefire and postfire watershed conditions under the February 1-9, 2024 precipitation event. This period consisted of two rainfall episodes separated by a short dry interval: an initial storm on February 1-2 followed by a more intense AR-driven event from February 4-7 and a subsequent rainfall pulse on February 8-9. These sequential storms generated two distinct flood peaks. The postfire response to these two peaks differed markedly (Fig. 5a and 5b). While the first peak exhibited only modest increases under postfire conditions (average +2.3%), the second peak showed systematically greater amplification, with increases averaging approximately +30%. This contrast suggests that postfire watershed changes exerted stronger influence during the later storm sequence. Such pattern is evident in the hydrographs (Fig. 5c) for Channels 24, 44, and 54, which are located immediately downstream of the burned area. In these channels, the postfire enhancement of the second peak is evident not only in relative terms but also in absolute

https://doi.org/10.5194/egusphere-2026-2665
Preprint. Discussion started: 13 July 2026

discharge magnitude. In contrast, the downstream Channel 84 shows a much weaker response, indicating attenuation of postfire effects with distance from the burned headwaters. Beyond peak flows, postfire conditions also increased runoff volume. The cumulative discharge increased by approximately 12%, 7%, and 15% in Channels 24, 44, and 54, respectively, compared to only a 1.3% increase in Channel 84. This indicates that wildfire-induced changes enhanced both the intensity and total runoff generation in areas directly connected to the burned landscape.

https://doi.org/10.5194/egusphere-2026-2665
Preprint. Discussion started: 13 July 2026

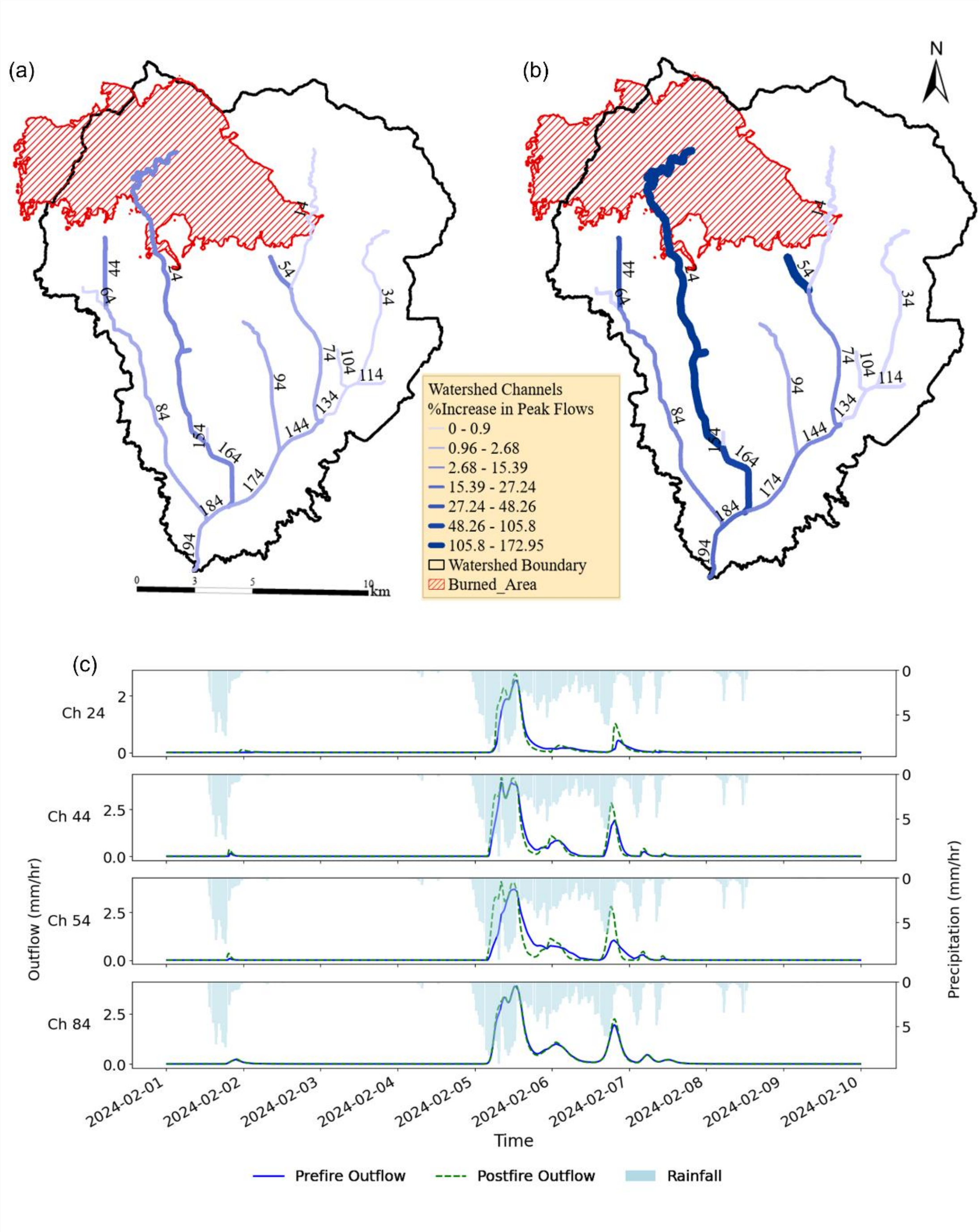

Figure 5: Postfire changes in peak flow and hydrograph response within the ESA watershed. Panels (a) and (b) show the percentage increase in the first and second flood peaks, respectively, across watershed channels under postfire conditions, with the red hatched area indicating the burned region. Channel colour and thickness represent the magnitude of peak-flow increase. Panel (c) compares simulated prefire and postfire hydrographs at four channels located downstream of the burned area. The blue solid line represents prefire outflow, while the green dashed line represents postfire outflow; rainfall is shown as light blue inverted bars.

https://doi.org/10.5194/egusphere-2026-2665
Preprint. Discussion started: 13 July 2026

Figure 6 presents the spatial distribution of relative differences in runoff generation between prefire and postfire conditions (postfire minus prefire) across hillslopes and channels within the ESA watershed. A clear spatial pattern emerges: areas in close proximity to the burned region exhibit substantially greater increases in runoff compared to more distal areas. Channels immediately downstream of the burned headwaters (Channels 24, 44, 54, and 94) show an average runoff increase of approximately 6% (weighted by drainage area), whereas the watershed-wide increase is about 2%. This downstream reduction reflects the progressive mixing of runoff contributions from unburned areas, which attenuates the localized postfire effect. At the hillslope scale, runoff response is highly heterogeneous, with increases ranging from roughly 1% to as high as 18% in areas adjacent to the burn scar. Notably, the strongest responses are confined to burned zones, indicating that wildfire-induced changes, such as reduced vegetation cover and enhanced soil water repellence, decreased infiltration and promoted greater surface runoff during the 2024 AR event.

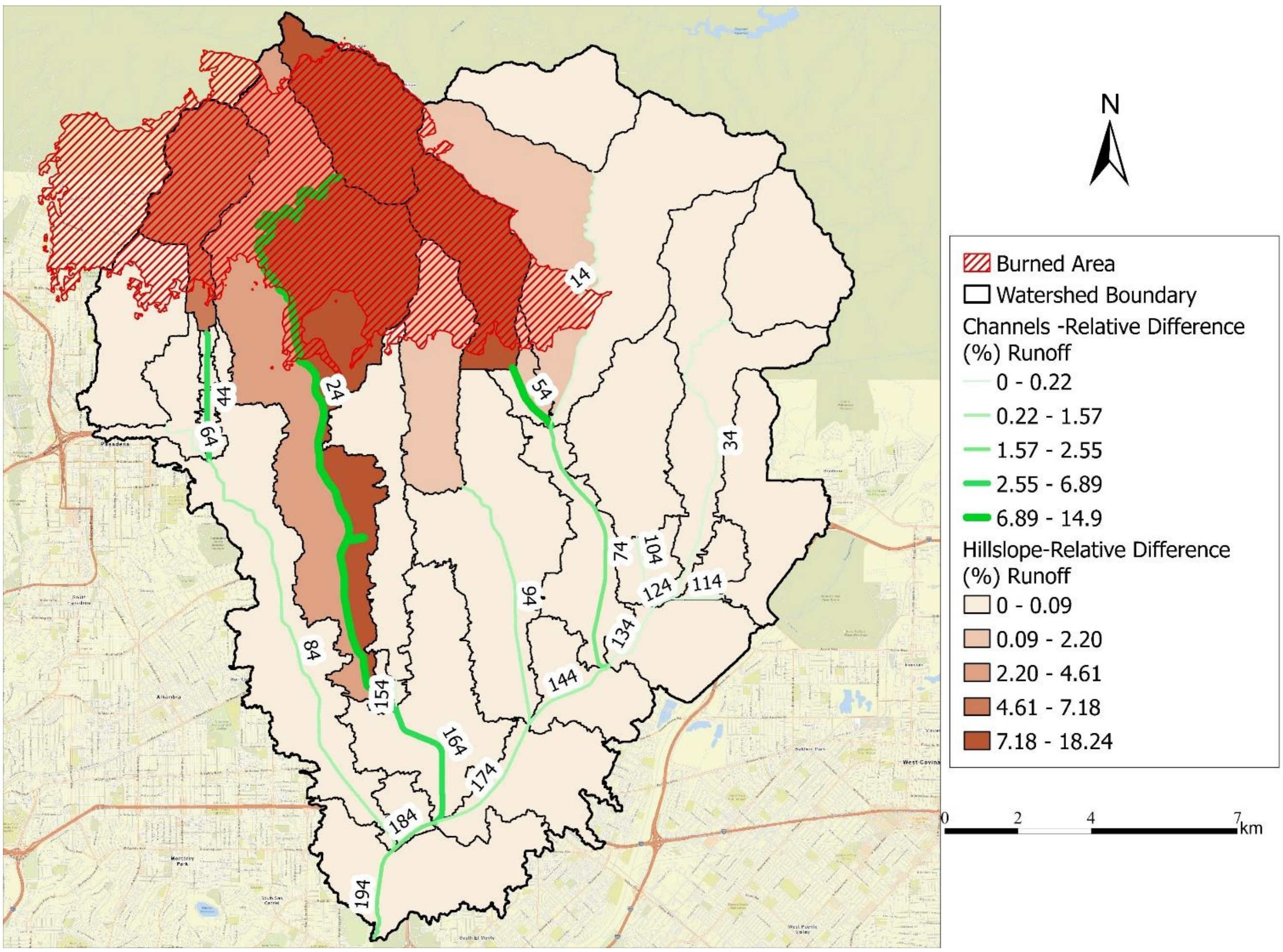

Figure 6: Relative difference (%) in runoff between prefire and postfire conditions for hillslopes and channels in the ESA watershed. The red hatched area denotes the burned region, and colour gradients indicate the magnitude of runoff change.

https://doi.org/10.5194/egusphere-2026-2665
Preprint. Discussion started: 13 July 2026

Figure 7 presents the relative difference (%) in sediment yield between prefire and postfire conditions across hillslopes and channels. The maximum increase reaches approximately 71% in channels and up to 112% in hillslopes. The spatial distribution of sediment yield changes broadly mirrors the runoff response shown in Fig. 6, with larger increases concentrated near the burned headwaters and progressively smaller changes downstream. Channels immediately below the burned area (Channels 24, 44, 54, and 94) exhibit an average increase of approximately 50% (area-weighted), compared to a watershed-wide increase of about 22%. Notably, the relative increase in sediment yield exceeds that observed for runoff volume. This reflects the compound effect of runoff on sediment transport through the concentration-discharge (C-Q) relationship, in which sediment concentration scales nonlinearly with flow. As a result, the sediment yield, being the product of runoff and sediment concentration, thus get further amplified. Mechanistically, the enhanced sediment yield near the burned region is linked to hillslope-scale erosion processes driven by vegetation loss, soil structure degradation, and increased soil water repellency. Further downstream, the postfire sediment signal is attenuated due to both dilution by runoff from unburned areas and in-channel deposition and temporary storage.

https://doi.org/10.5194/egusphere-2026-2665
Preprint. Discussion started: 13 July 2026

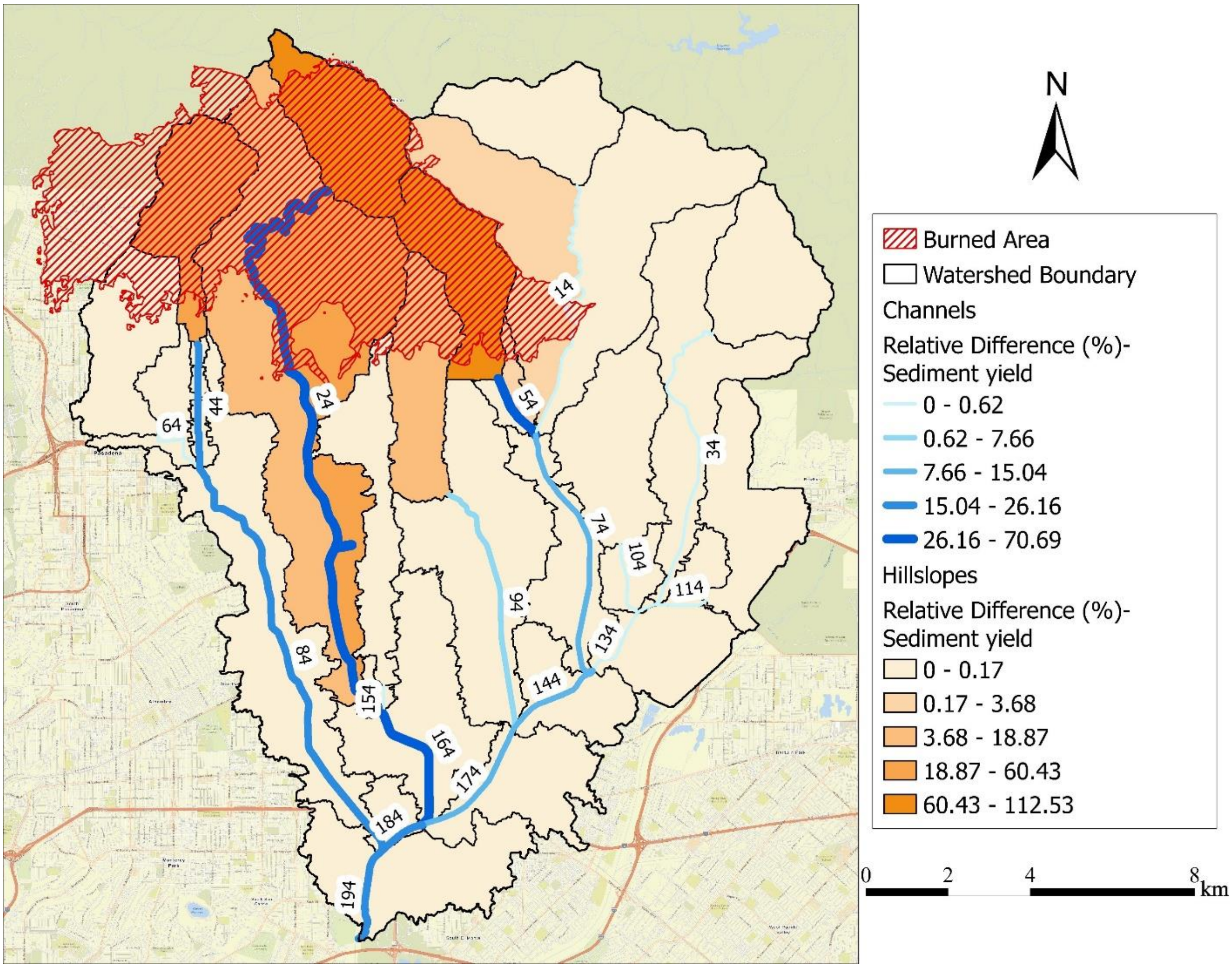

Figure 7: Relative difference (%) in sediment yield between prefire and postfire conditions across hillslopes and channels in the ESA watershed. The red hatched area indicates the burned region, and colour gradients represent the magnitude of sediment yield increase.

4 Discussion

This section interprets the modelled hydrologic responses within a broader compound hazard framework involving wildfire and atmospheric river (AR) interactions. We first examine how storm duration influences postfire runoff amplification, using historical AR records to contextualize the 2024 event. We then discuss key sources of modelling uncertainty and their implications for interpreting runoff and sediment responses. Finally, we explore future research directions that consider the bidirectional coupling between ARs and wildfire as mutually reinforcing drivers of flood and erosion risk.

https://doi.org/10.5194/egusphere-2026-2665
Preprint. Discussion started: 13 July 2026

4.1 Impact of Atmospheric Event Duration on Runoff

As shown in Fig. 5, postfire flood response is influenced not only by rainfall intensity but also by event duration, as prolonged precipitation progressively fills surface and subsurface storage and reduces attenuation capacity for subsequent runoff peaks. To further investigate this effect, we examined the historical duration of AR events (Scale ≥ 3) across the five Southern California locations (points A-E in Fig. 3a) using the CW3E dataset. Figure 8a presents the distribution of AR event durations over the 64-year record (1960-2024), comprising 169 events with durations ranging from approximately 20 to 120 hours. Most events persist for 50-60 hours, with a near-symmetric distribution reflected by the close agreement between the mean (55.2 hours) and median (54 hours).

In comparison, the February 2024 AR event exhibited a maximum duration of 36 hours across the five locations, corresponding to the primary rainfall episode from 4-6 February that generated the dominant hydrograph response (Fig. 5c), with additional precipitation occurring before and after this core period. Because AR classification in the CW3E dataset is based on threshold exceedance of vertically integrated water vapor transport (IVT)(Ralph et al., 2019), this 36-hour window captures the peak moisture transport phase of the event. Only 17% of historical AR ≥ 3 events had shorter durations than the 2024 event (Fig. 8b), indicating that 83% of comparable events lasted longer and could impose greater hydrologic loading. When considered alongside the frequency and recurrence analysis (Sect. 3.1), this suggests that not only is the occurrence of a postfire AR event plausible, but future events may also have longer durations than the one simulated here, potentially leading to even greater flood impacts.

https://doi.org/10.5194/egusphere-2026-2665
Preprint. Discussion started: 13 July 2026

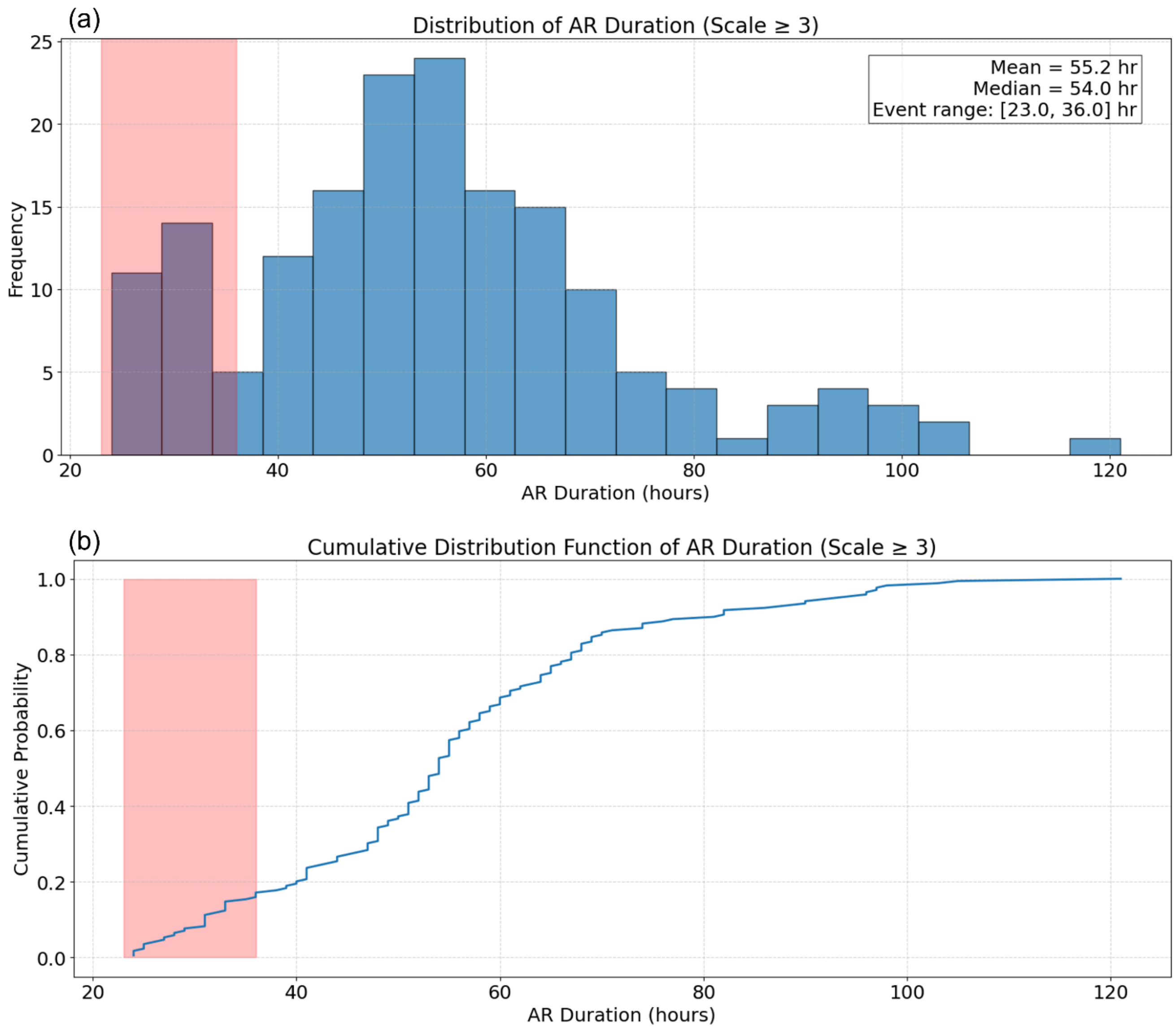

Figure 8: Histogram (a) and cumulative distribution function (b) of the duration of AR events with Scale ≥ 3 in Southern California based on the historical CW3E record. Event durations range from approximately 25 to 120 hours across 169 events identified at the five study locations

4.2 Sources of Uncertainty

This study provides estimates of runoff and sediment yield under prefire and postfire conditions during an extreme AR event. In the prefire scenario, the simulation effectively reconstructs the hydrologic response to the February 2024 AR event. These results offer spatially continuous insight into watershed behaviour in a system where functional hydrologic observations are limited. Despite inherent modelling uncertainties, the simulated runoff response is consistent with observed behaviour in a

https://doi.org/10.5194/egusphere-2026-2665
Preprint. Discussion started: 13 July 2026

neighbouring watershed (Fig. 4). These results are particularly meaningful because of the continuity in space and time, whereas functional hydrologic observations are non-existent in the study watershed thus prohibits any characterization of the flood hazard. Furthermore, the spatial patterns of postfire response (Fig.6 and Fig.7) showing stronger impacts near burned areas and attenuation downstream align with previous findings that wildfires exert the greatest hydrological influence locally before diminishing toward the watershed outlet due to spatial averaging and transmission losses(Sidman et al., 2016; Havel et al., 2018). Similarly, the amplified second flood peak observed in this study (Fig. 5) is consistent with prior work documenting delayed but enhanced postfire storm responses(Nasirzadehdizaji and Akyuz, 2022; Dilshan et al., 2025).

Nevertheless, several sources of uncertainty should be acknowledged. First, the absence of in-watershed streamflow observations limits calibration and validation. As discussed in Sect. 2.5, model calibration was constrained to total event runoff volumes, meaning that simulated peak flow magnitudes and timing retain greater uncertainty. Second, representation of postfire landscape changes is simplified. Ideally, wildfire effects would be modelled through detailed adjustments to interception, infiltration, and overland flow processes(Sidman et al., 2016). In KINEROS2, however, postfire impacts are approximated through modifications to a limited set of parameters, including land cover characteristics, interception, and hydraulic conductivity. While such parameterizations are widely used and form part of established AGWA/KINEROS2 workflows adopted by management agencies(Semmens et al., 2007; Goodrich et al., 2012), they inevitably simplify the full complexity of postfire hydrologic change. Finally, structural limitations of KINEROS2 introduce additional uncertainty in sediment estimates. The model primarily represents hillslope sheet and rill erosion and channel transport processes and does not explicitly simulate soil loss mechanisms such as landslides or debris flows. Because such processes contributed significantly to sediment export during the 2024 AR event(Selby, 2025), sediment yield may be.

4.3 Compound AR-Wildfire Interactions and Future Research Needs

While this study focuses on the postfire flood amplification associated with an AR event following wildfire, an equally important cascading pathway operates in the reverse direction: antecedent AR events may precondition landscapes for subsequent wildfire occurrence(Albano et al., 2017). For example, February 2024 AR likely enhanced vegetation growth through increased soil moisture, which contributed to elevated fuel loads preceding the 2025 Eaton Fire after an extended period of hot and dry conditions. Given the demonstrated frequency and recurrence of AR events in Southern California, such AR-fire linkages may represent a recurring hazard sequence rather than isolated occurrences. This suggests a coupled hazard cycle in which AR events promote fuel accumulation that increases wildfire susceptibility, while wildfire-induced soil and vegetation changes subsequently enhance flood and erosion risks during later AR-driven storms. In this framework, wildfire and AR events interact not as independent disturbances but as mutually reinforcing processes that shape regional hydrologic and geomorphic responses.

Future research should examine how this bidirectional cascade is influenced by hydrometeorological variables such as soil moisture memory, temperature extremes, atmospheric humidity, and Santa Ana wind patterns. Previous studies have noted that interactions between ARs and Santa Ana winds may increase both wildfire likelihood and the severity of subsequent

https://doi.org/10.5194/egusphere-2026-2665
Preprint. Discussion started: 13 July 2026

hydrologic extremes(Guirguis et al., 2023). Advancing understanding of these coupled processes could improve multi-hazard risk assessment and inform more integrated forecasting and mitigation strategies.

5 Conclusion

This study examined the cascading hydrologic impacts that may arise when an extreme Atmospheric River (AR) event follows a major wildfire, using the 2025 Eaton Fire as a representative case. By integrating historical AR climatology with event-based hydrologic modelling, we quantified how wildfire-induced landscape changes could amplify runoff generation and sediment transport under a plausible postfire storm scenario.

Our analysis indicates that strong AR events (Scale ≥ 3) occur with a mean annual frequency of approximately 0.51 along the Southern California coast, with a 38% probability of recurrence in consecutive years. This supports the plausibility of a severe AR analogous to the February 2024 event to occur in the year following a major wildfire such as the Eaton Fire. Under such conditions, postfire hydrologic responses were found to intensify near burned headwaters, where runoff volume increased by about 6% and sediment yield by approximately 50% in channels immediately downstream of the burned area. Sequential storm pulses during the February 2024 AR event produced two flood peaks, with the second peak exhibiting substantially greater postfire amplification (≈30%) compared to the first (≈2%), reflecting reduced watershed storage following antecedent runoff. Historical records further suggest that ARs often persist longer than the 2024 event simulated here, implying that future postfire storms may pose even greater flood risk.

Beyond these event-scale findings, a broader compound hazard dynamic needs to be better understood in future studies. Wildfire alters infiltration capacity and vegetation structure, increasing susceptibility to subsequent hydrologic extremes, while AR events can both precondition wildfire through fuel accumulation and trigger postfire flooding. Together, these processes shape watershed-scale flood risk in ways that cannot be understood by examining either hazard in isolation. Recognizing this coupling is critical for postfire risk assessment, emergency preparedness, and watershed management in fire-prone regions. Future work should further examine the bidirectional interactions between AR-driven moisture variability and wildfire susceptibility to better anticipate cascading hydrologic risks under a changing climate.

Author contributions

All authors contributed to the study conception and design. Fehmida Rafi contributed to data analysis, modelling, and writing of the original draft of the manuscript. Daniel Rowland contributed to modelling and editing the manuscript. Shang Gao contributed to the conceptualization, design, editing of the manuscript, and funding acquisition.

https://doi.org/10.5194/egusphere-2026-2665
Preprint. Discussion started: 13 July 2026

Competing interests

The authors declare that they have no conflict of interest.

Acknowledgements

We gratefully acknowledge scientists at USDA-ARS including Haiyan Wei, Carl Unkrich, and David Goodrich who provided valuable help and insights on hydro-modeling. During the preparation of this work, the authors used ChatGPT (OpenAI) to assist with language refinement and manuscript polishing. After using this tool, the authors reviewed and edited the content as needed and take full responsibility for the content of the published article.

Financial support

This research is mainly funded by start-up funding from the University of Arizona to Shang Gao and partially by USDA via Agreement NR213A750023C013 to Shang Gao. Fehmida Rafi was partially supported by the Fulbright Program.

References

Abatzoglou, J., Kolden, C., Williams, A., Sadegh, M., Balch, J., and Hall, A.: Downslope wind-driven fires in the Western United States, Earth's Future, 11, e2022EF003471, https://doi.org/10.1029/2022EF003471, 2023.

AghaKouchak, A., Huning, L. S., Chiang, F., Sadegh, M., Vahedifard, F., Mazdiyasni, O., Moftakhari, H., and Mallakpour, I.: How do natural hazards cascade to cause disasters?, Nature, 561, 458–460, 2018.

Albano, C. M., Dettinger, M. D., and Soulard, C. E.: Influence of atmospheric rivers on vegetation productivity and fire patterns in the southwestern US, Journal of Geophysical Research: Biogeosciences, 122, 308–323, https://doi.org/10.1002/2016JG003608, 2017.

NOAA Analysis of Record for Calibration (AORC) Dataset https://registry.opendata.aws/noaa-nws-aorc, last access: February 27.

BAER Imagery Support Data Download: https://burnseverity.cr.usgs.gov/baer/baer-imagery-support-data-download, last access: February 27.

Carlson, A. R., Hawbaker, T. J., Mockrin, M. H., Radeloff, V. C., Bair, L. S., Caggiano, M. D., Meldrum, J. R., Alexandre, P. M., Kramer, H. A., and Steblein, P. F.: Rising rates of wildfire building destruction in the conterminous United States, Proceedings of the National Academy of Sciences, 122, e2505886122, https://doi.org/10.1073/pnas.2505886122, 2025.

Cobb, A., Ralph, F. M., Tallapragada, V., Wilson, A. M., Davis, C. A., Monache, L. D., Doyle, J. D., Pappenberger, F., Reynolds, C. A., and Subramanian, A.: Atmospheric river reconnaissance 2021: A review, Weather and Forecasting, https://doi.org/10.1175/WAF-D-21-0164.1, 2022.

Corringham, T. W., McCarthy, J., Shulgina, T., Gershunov, A., Cayan, D. R., and Ralph, F. M.: Climate change contributions to future atmospheric river flood damages in the western United States, Scientific Reports, 12, 13747, https://doi.org/10.1038/s41598-022-15474-2, 2022.

Dilshan, W., Hiraga, Y., and Kazama, S.: Wildfire-Induced Enhancement in Downstream Flood Discharge in Watersheds of California, Journal of Flood Risk Management, 18, e70054, https://doi.org/10.1111/jfr3.70054, 2025.

Duane, A., Castellnou, M., and Brotons, L.: Towards a comprehensive look at global drivers of novel extreme wildfire events, Climatic Change, 165, 43, https://doi.org/10.1007/s10584-021-03066-4, 2021.

Gershunov, A., Shulgina, T., Ralph, F. M., Lavers, D. A., and Rutz, J. J.: Assessing the climate-scale variability of atmospheric rivers affecting western North America, Geophysical Research Letters, 44, 7900–7908, https://doi.org/10.1002/2017GL074175, 2017.
Goodrich, D., Burns, I., Unkrich, C., Semmens, D. J., Guertin, D., Hernandez, M., Yatheendradas, S., Kennedy, J. R., and Levick, L. R.: KINEROS2/AGWA: Model use, calibration, and validation, Transactions of the ASABE, 55, 1561–1574, 2012.
Soil Survey Staff. Gridded Soil Survey Geographic (gSSURGO) Database for California. United States Department of Agriculture, Natural Resources Conservation Service. : https://gdg.sc.egov.usda.gov/, last access: February 27.
Guirguis, K., Gershunov, A., Hatchett, B., Shulgina, T., DeFlorio, M. J., Subramanian, A. C., Guzman-Morales, J., Aguilera, R., Clemesha, R., and Corringham, T. W.: Winter wet–dry weather patterns driving atmospheric rivers and Santa Ana winds provide evidence for increasing wildfire hazard in California, Climate Dynamics, 60, 1729–1749, https://doi.org/10.1007/s00382-022-06361-7, 2023.
Havel, A., Tasdighi, A., and Arabi, M.: Assessing the hydrologic response to wildfires in mountainous regions, Hydrology and Earth System Sciences, 22, 2527–2550, https://doi.org/10.5194/hess-22-2527-2018, 2018.
Keeley, J. E. and Syphard, A. D.: Large California wildfires: 2020 fires in historical context, Fire Ecology, 17, 22, https://doi.org/10.1186/s42408-021-00110-7, 2021.
Keeley, J. E., Guzman-Morales, J., Gershunov, A., Syphard, A. D., Cayan, D., Pierce, D. W., Flannigan, M., and Brown, T. J.: Ignitions explain more than temperature or precipitation in driving Santa Ana wind fires, Science advances, 7, eabh2262, https://doi.org/10.1126/sciadv.abh2262, 2021.
Kelley, D. I., Burton, C., Di Giuseppe, F., Jones, M. W., Barbosa, M. L. F., Brambleby, E., McNorton, J. R., Liu, Z., Bradley, A. S. I., Blackford, K., Burke, E., Ciavarella, A., Di Tomaso, E., Eden, J., Ferreira, I. J. M., Fiedler, L., Hartley, A. J., Keeping, T. R., Lampe, S., Lombardi, A., Mataveli, G., Qu, Y., Silva, P. S., Spuler, F. R., Steinmann, C. B., Torres-Vázquez, M. Á., Veiga, R., Van Wees, D., Wessel, J. B., Wright, E., Bilbao, B., Bourbonnais, M., Gao, C., Di Bella, C. M., Dintwe, K., Donovan, V. M., Harris, S., Kukavskaya, E. A., N'Dri, A. B., Santín, C., Selaya, G., Sjöström, J., Abatzoglou, J. T., Andela, N., Carmenta, R., Chuvieco, E., Giglio, L., Hamilton, D. S., Hantson, S., Meier, S., Parrington, M., Sadegh, M., San-Miguel-Ayanz, J., Sedano, F., Turco, M., Van Der Werf, G. R., Veraverbeke, S., Anderson, L. O., Clarke, H., Fernandes, P. M., and Kolden, C. A.: State of Wildfires 2024–2025, Earth System Science Data, 17, 5377–5488, 10.5194/essd-17-5377-2025, 2025.
Kumar, M., AghaKouchak, A., Abatzoglou, J. T., and Sadegh, M.: Compounding effects of climate change and WUI expansion quadruple the likelihood of extreme-impact wildfires in California, Natural Hazards, 2, 17, https://doi.org/10.1038/s44304-025-00067-6, 2025.
Miller, J., Touma, D., and Brunner, M. I.: Compounding preconditions of wildfires vary in time and space within Europe, Communications Earth & Environment, 6, 1005, https://doi.org/10.1038/s43247-025-02955-1, 2025.
Moazeni, S. and Cerdà, A.: The impacts of forest fires on watershed hydrological response. A review, Trees, Forests and People, 18, 100707, https://doi.org/10.1016/j.tfp.2024.100707, 2024.
Multi-Resolution Land Characteristics (MRLC) Consortium https://www.mrlc.gov/viewer/, last access: February 27.
Nasirzadehdizaji, R. and Akyuz, D. E.: Predicting the potential impact of forest fires on runoff and sediment loads using a distributed hydrological modeling approach, Ecological Modelling, 468, 109959, 2022.
Papaioannou, G., Alamanos, A., and Maris, F.: Evaluating post-fire Erosion and flood protection techniques: a narrative review of applications, GeoHazards, 4, 380–405, https://doi.org/10.3390/geohazards4040022, 2023.
Phillips, S.: The Palisades and Eaton Fires: Neighborhood Data and Potential Housing Market Effects, 2025.
Prats, S. A., Malvar, M. C., and Wagenbrenner, J. W.: Compaction and cover effects on runoff and erosion in post-fire salvage logged areas in the Valley Fire, California, Hydrological Processes, 35, e13997, https://doi.org/10.1002/hyp.13997, 2021.
Qing, Y., Wang, S., Yang, Z.-L., and Gentine, P.: Soil moisture− atmosphere feedbacks have triggered the shifts from drought to pluvial conditions since 1980, Communications Earth & Environment, 4, 254, https://doi.org/10.1038/s43247-023-00922-2, 2023.
Ralph, F. M., Rutz, J. J., Cordeira, J. M., Dettinger, M., Anderson, M., Reynolds, D., Schick, L. J., and Smallcomb, C.: A scale to characterize the strength and impacts of atmospheric rivers, Bulletin of the American Meteorological Society, 100, 269–289, https://doi.org/10.1175/BAMS-D-18-0023.1, 2019.
Samburova, V., Schneider, E., Rüger, C. P., Inouye, S., Sion, B., Axelrod, K., Bahdanovich, P., Friederici, L., Raeofy, Y., and Berli, M.: Modification of soil hydroscopic and chemical properties caused by four recent California, USA megafires, Fire, 6, 186, https://doi.org/10.3390/fire6050186, 2023.

Selby, W.: Atmospheric River: Friend or Foe?, Weatherwise, 78, 17–27, https://doi.org/10.1080/00431672.2025.2431446, 2025.

Semmens, D., Goodrich, D., Unkrich, C., Smith, R., Woolhiser, D., and Miller, S.: KINEROS2 and the AGWA modelling framework, Hydrological modelling in arid and semi-arid areas, 49, 2007.

Sidman, G., Guertin, D. P., Goodrich, D. C., Thoma, D., Falk, D., and Burns, I. S.: A coupled modelling approach to assess the effect of fuel treatments on post-wildfire runoff and erosion, International Journal of Wildland Fire, 25, 351–362, https://doi.org/10.1071/WF14058, 2016.

United States Geological Survey https://apps.nationalmap.gov/downloader/, last access: February 27.

Monitoring location - Arroyo Seco NR Pasadena CA - USGS-11098000: https://waterdata.usgs.gov/monitoring-location/USGS-11098000/#dataTypeId=continuous-00065-0&period=P7D&showFieldMeasurements=true, last access: February 27.